

# Effect of Warm Rolling Process Parameters on Microstructure and Mechanical Properties of Structural Steels

Suman Kant Thakur<sup>1</sup>  · Alok Kumar Das<sup>2</sup> · Bimal Kumar Jha<sup>3</sup>

Received: 3 September 2021 / Accepted: 31 December 2021 / Published online: 5 February 2022  
© The Indian Institute of Metals - IIM 2022

**Abstract** Warm rolling has grown interest as means of cutting down costs and of extending the application range of hot-rolled products. However, high resistance to deformation limits its application. Warm rolling is presently not in practice for carbon steel rolling in any of the SAIL plants. In view of this, the feasibility of warm rolling of structural steels, namely E250/E350/E450 steel grades, was conducted in the Experimental Rolling Mill to evaluate the effect of warm rolling parameters on deformation behavior, microstructure and properties of structural steel. The deformation temperature range was determined using JMatPro software for carrying out warm rolling of the selected grade of steels. Processing maps were also constructed to determine the safe working window for warm rolling. The microstructure of warm-rolled samples dominates fragmented Pearlite with elongated ferrite. Decrease in temperature results in more fragmented pearlite in the microstructure. The increased ratio of fragmented pearlite in microstructure leads to higher strength in structural steels. Improvement in yield strength and tensile strength by more than 12% with same toughness in properties is observed for warm-rolled sample compared to the conventional hot-rolled sample. From the results, it is inferred

that warm rolling can be used to achieve better mechanical properties with the same alloy chemistry.

**Keywords** Warm rolling · Microstructure · Micro-alloyed steel · Tensile strength · Deformation

## 1 Introduction

Conventionally hot rolling is performed above Ar<sub>3</sub> temperature, i.e., temperature at which austenite begins to transform to ferrite during cooling. Rolling between phase transformation temperature, i.e., Ar<sub>3</sub> and Ar<sub>1</sub> temperature and below Ar<sub>1</sub> (the temperature at which transformation of austenite to ferrite or ferrite plus cementite is completed) are termed as warm rolling. Warm rolling entails ferrite deformation, the temperature at which the phase changes from austenite to ferrite occurs. Warm rolling is often carried out below Ar<sub>1</sub> temperature such that the microstructure during the final finishing passes is composed of fragmented pearlite and elongated ferrite. This requires reducing the temperatures of the complete rolling schedule from 1250–850 °C to 800–700 °C. It is to be noted that rolling at a lower temperature regime requires a higher-powered mill. The workpiece undergoes transformation from the FCC austenite phase to the BCC ferrite phase during two phase rolling. During warm rolling, the pearlite is converted into fragmented pearlite and there is a significant impact on the final microstructures and that improves mechanical properties.

Many researchers have published their work on warm rolling. Hu et al. found that the warm rolling process can effectively promote the cementite precipitation and produce retained austenite grains having both equiaxed and lamellar morphologies in 7%Mn steel, leading to a

✉ Suman Kant Thakur  
skthakur@sail.in

Alok Kumar Das  
alokmech@iitism.ac.in

Bimal Kumar Jha  
bimalkjha104@gmail.com

<sup>1</sup> R&D Centre for Iron and Steel, Steel Authority of India Ltd., Ranchi 834002, India

<sup>2</sup> IIT(ISM), Dhanbad 826004, India

<sup>3</sup> NIFFT, Ranchi 834003, India

simultaneous improvement in both strength and ductility [1]. In another paper [2], Bin Hu et al. discussed the design strategy by combining the warm rolling process with V alloying to develop super-high-strength medium Mn steel with good ductility. Han Zheng et al. in their paper discussed the combination of heavy warm rolling of the metastable austenite and subsequent quenching, tempering to produce ultrahigh-strength steel [3]. They achieved the yield strength, ultimate tensile strength as 1911 MPa and 2411 MPa respectively by following warm rolling and quenching process, compared to 1612 MPa and 1852 MPa by conventional severe plastic deformation (SPD) rolling. In another work by Tadanobu Inoue et al. [4], 800 MPa class 0.15%C-0.3%Si-1.5%Mn steel bar with ultrafine elongated grain structures of transverse grain size 1.2  $\mu\text{m}$  was developed using multi-pass bi-axial rolling process at a warm working temperature. The developed steel had a distribution of strong texture leading to improved strength–toughness balance. The advanced thermo-mechanical processing routes also utilize large-strain warm deformation to produce high-strength steel [5]. Bo Gao et al. reported an ultra-strong (2.15 GPa) low-carbon nano-steel processed by hetero-structure and interstitial mediated warm rolling [6].

The developed nano-steel consisted of thin ( $\sim 17.8$  nm) lamellae, which was achieved by adjusting the warm rolling temperature. Shen et al. followed warm rolling in plate rolling which is more suitable for industrial production to develop high strength and high toughness steels [7]. To reduce deformation resistance, warm rolling was carried out in the dual-phase region. The study suggests that warm rolling can greatly enhance strength by  $\sim 64$ –158 MPa compared to the conventional controlled rolling process. Sergeev et al. [8] studied the effect of warm rolling on the structure and mechanical properties of the low-carbon pipe steel. They concluded that the warm rolling resulted in the formation of an anisotropic ultrafine-grained structure with average grain/sub-grain size 0.5  $\mu\text{m}$  in the transverse direction and 20–30  $\mu\text{m}$  along the rolling direction leading to significant improvement in low-temperature toughness. Kim et al. have affirmed that warm rolling under conditions of deformation is a very efficient way to enhance the mechanical properties of the alloys and metals [9]. Satish Kumar et al. developed an industrial warm rolling process for the IF grade steel through plant trials in a seven-stand hot strip mill under a warm regime for producing an intermediate product, a hard cold strip for subsequent cold rolling and annealing [10].

In the present work, the effect of warm rolling parameters on deformation behavior, microstructure and properties of structural steel namely E250/E350/E450 grades were evaluated. The study involved rolling steel samples at Experimental Rolling Mill (ERM) at different rolling temperatures. The evolution of microstructure during warm

rolling and its influence on mechanical properties have also been studied. It has been observed that the effect of warm rolling is more at lower temperature and leads to more elongated ferrite, fragmented pearlite with finer spheroidal cementite, leading to better mechanical properties.

## 2 Experimental

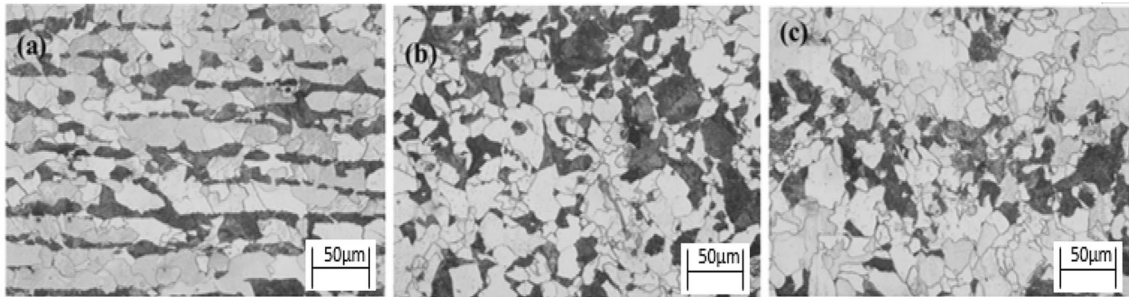
The experimental study mainly involved warm rolling and subsequent metallographic examination along with mechanical testing of steels. To carry out warm rolling experiments, plate samples of structural steel, namely E250/E350/E450 steel were collected from Plate Mill, Rourkela Steel Plant. The thickness of the collected plate samples was 25 mm. Chemical analysis of the collected samples was carried out using Optical Emission Spectroscopy (OES). The elemental composition of the samples is shown in Table 1. The microstructure of as-received samples is shown in Fig. 1.

Figure 1 shows the microstructure of plates, obtained at a magnification of 500X. The microstructure of E250 grade steels contains typical ferrite and pearlite with grain size around 25  $\mu\text{m}$ . The microstructure of E350 and E450 reveal refined grain structure compared to E250 grade steel and grain size found in the range of 15–20  $\mu\text{m}$ . The grains in micro-alloyed steels are more refined due to Nb and Ti precipitates during hot rolling which hinders grain coarsening due to the pinning effect.

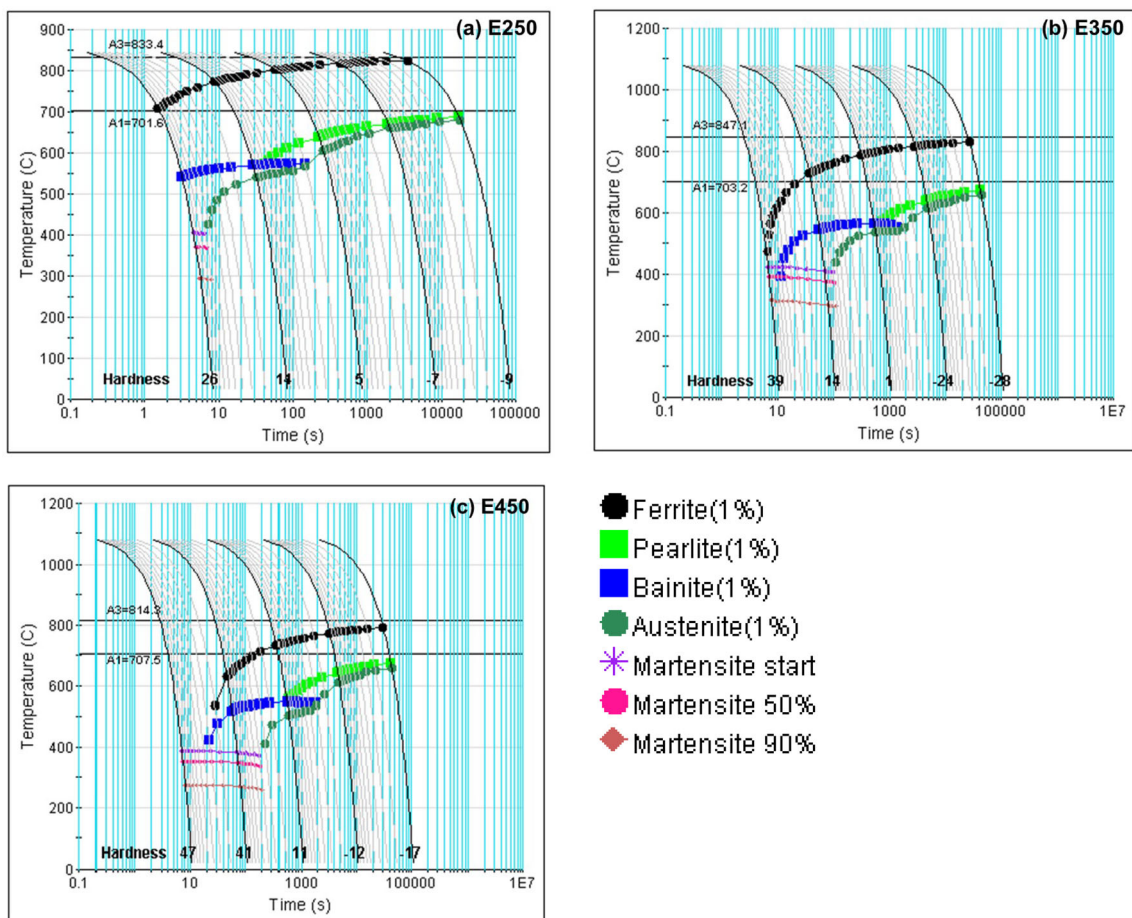
The Continuous Cooling Transformation (CCT) curves for the experimental steels were generated using JMatPro software, shown in Fig. 2. The critical temperatures, i.e., austenite start ( $A_1$ ) and austenite finish ( $A_3$ ) during heating for each grade were taken from CCT curves. The temperature interval between  $A_1$  and  $A_3$  temperatures is the critical range in which the austenite exists in equilibrium with ferrite.  $A_1$  &  $A_3$  temperature determined using CCT curves for an identified grade is shown in Table 2. The reason for the relatively low  $A_3$  temperature of E450 can be attributed to high carbon content. The flow stress data of all the three grades were also generated using JMatPro software for a strain rate of  $10^{-3}$ – $100$   $\text{s}^{-1}$  and temperature range of 500–900  $^\circ\text{C}$  to construct deformation map. Deformation maps were also used to ascertain the selected warm rolling parameters for all three grades. Warm rolling of steel samples was conducted in ERM. ERM is a single stand reversing mill with a roll diameter of 350 mm and 400 mm barrel length. Details of experiments carried out at ERM are shown in Fig. 3. The plates were initially reheated to 1150  $^\circ\text{C}$  and soaked for 120 min. After that, the furnace temperature was reduced to deformation temperature and soaked for 30 min. Thereafter, the plate samples were rolled in five passes at ERM to achieve a total reduction of

**Table 1** Chemical analysis of selected grade of steel (wt%)

Grade	C	Si	Mn	P	S	Al	Nb	Ti	V	N
E250	0.14	0.27	1.30	0.024	0.0052	0.027	–	–	–	0.006
E350	0.14	0.26	1.28	0.034	0.034	0.033	0.056	0.019	–	0.009
E450	0.21	0.24	1.46	0.016	0.011	0.023	0.049	0.019	0.043	0.0091



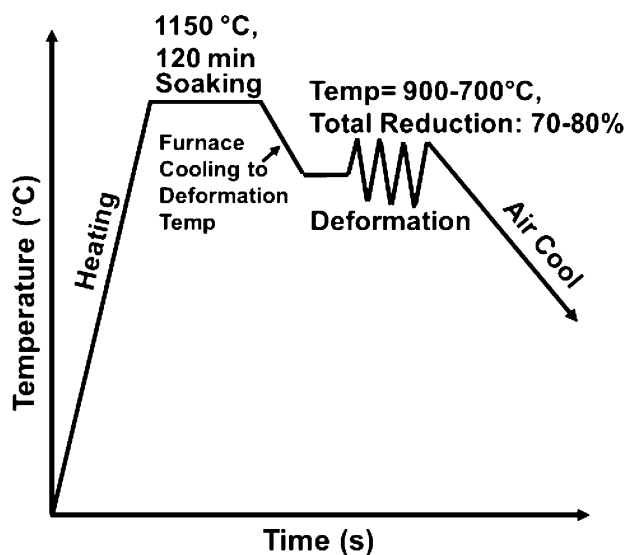
**Fig. 1** Microstructure of as received samples **a** E250, **b** E350, **c** E450



**Fig. 2** CCT Curves of Experimental Steel generated using JMatPro **a** E250, **b** E350, **c** E450

**Table 2** Determination of A1 & A3 temperature in JMatPro

	E250	E350	E450
A <sub>3</sub> (°C)	833.4	847.1	814.3
A <sub>1</sub> (°C)	701.6	703.2	707.5

**Fig. 3** Schematic Diagram of Experiments carried out at ERM

more than 70% and the final thickness of plates was 5 mm. A maximum reduction of 36% (25–16 mm) was given in the first pass and an equal reduction of 25% was given in

the remaining four passes to achieve a final thickness of 5 mm. The temperature after each pass is shown in Table 3. The effective strain during rolling pass was 0.25–0.5 and the average strain rate varied between 15 and 30 s<sup>-1</sup>. The effect of lower deformation temperature on mill load was evaluated by comparing roll force. The effect of warm rolling on material properties was also evaluated. After rolling, the samples were prepared for the metallographic examination and mechanical testing evaluation.

The microstructural analysis was performed carried out using DM600 M Leica Optical Microscope. The polished surfaces of the samples were etched in 2% Nital (3% nitric acid + 97% ethanol) solution. The grain size measurement was performed by the mean linear intercept method (ASTM E112-12). The Scanning Electron Microscopy (SEM) was done using a field emission scanning electron microscope (FE-SEM, ZEISS ULTRA 55), operated at 15 kV. The Electron Back-Scattered Diffraction (EBSD) technique was used to mainly observe the low-angle and high-angle grain boundaries to find the impact of warm rolling temperature on strength and toughness values. The deformed samples, after polishing by colloidal Silica suspension, were investigated through the use of EBSD

**Table 3** Temperature during warm rolling

Sl no.	Grade	Pass number				
		1	2	3	4	5
1	E450	800	786	775	765	755
2	E450	770	757	748	736	728
3	E450	750	735	725	710	700
4	E450	725	720	709	703	690
5	E450	710	698	690	682	676
6	E350	900	890	875	860	850
7	E350	800	785	770	758	745
8	E350	760	750	745	730	715
9	E350	730	720	710	692	680
10	E350	710	695	690	680	670
11	E250	800	784	776	750	740
12	E250	780	770	755	745	730
13	E250	755	740	727	716	710
14	E250	740	725	717	705	695
15	E250	710	685	680	667	664

operating at an acceleration voltage of 20 keV and  $500 \times$  magnification. The role of precipitates during warm rolling was studied by Thermo-Calc and TEM analysis. TEM characterizations were performed with a Philips CM 200 FEG electron microscope using an accelerating voltage of 200 kV. The tensile test was performed to evaluate the tensile strength at room temperature in the universal tensile testing machine (Instron 1195). Samples for the tensile test were prepared with gauge length: 50 mm and width: 12.5 mm from the warm-rolled plates. The tensile test was also used to determine the  $r$ -value in samples in directions of  $0^\circ$ ,  $45^\circ$ , and  $90^\circ$  from the longitudinal direction. The displacements in longitudinal and transverse directions were recorded during the experiment in all samples. The initial and final sample dimensions are shown in Fig. 4.

The CVN impact toughness test was conducted using an impact testing machine (Tinius Olsen), and the average value was calculated after three measurements. Tensile and CVN Impact toughness was conducted according to ASTM E8/E8M-13a and ASTM E23 standards, respectively.

### 3 Results and Discussions

#### 3.1 JMatPro Analysis

The JMatPro version 10.2 software has been used to calculate the material properties of the selected grades of steel. Critical temperatures determined using CCT and TTT diagram are already shown in Table 2. Further, phase volume was determined using JmatPro by austenising the steel from room temperature to  $900^\circ\text{C}$  at a heating rate of

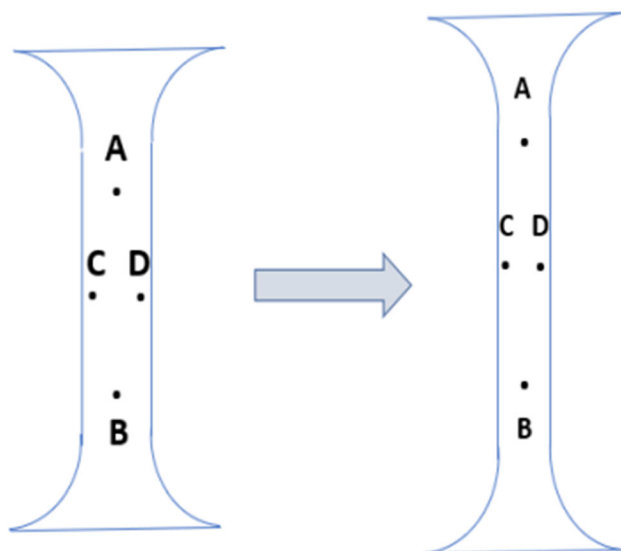


**Fig. 4** A, B, C, and D points marked on the original sample and corresponding points on the tensile specimen surface after the test

$1^\circ\text{C/s}$  as shown in Fig. 5. Figure 5 indicates the variation of ferrite and austenite content with respect to temperature. Normally warm rolling of plates is done such that the microstructure during finish rolling is composed of more than 90% ferrite. The rolling temperature for more than 90% ferrite in the microstructure is determined from Fig. 5 and found to be  $780^\circ\text{C}$ ,  $760^\circ\text{C}$ , and  $750^\circ\text{C}$  for E250, E350, and E450, respectively.

#### 3.2 Thermo-Calc Analysis

Thermo-Calc analysis was done for finding the start, finish and variation of precipitates in E350 (Nb–Ti) and E450 (Nb–V–Ti) micro-alloyed steels with respect to temperature. The graphs showing the amount of all phases with respect to temperature are shown in Fig. 6. From the graph plotted through Thermo-Calc 2019b for both types of micro-alloyed steels, it is clear that the Nb precipitates are formed in both grades. However, in E450, the precipitates of VC are found to be more than the Nb, Ti(C, N) precipitates. Later, it has also been confirmed that the precipitations of Nb, Ti(C, N), and VC are found in E450 (Nb–V–Ti) micro-alloyed steels through EDS analysis in TEM.

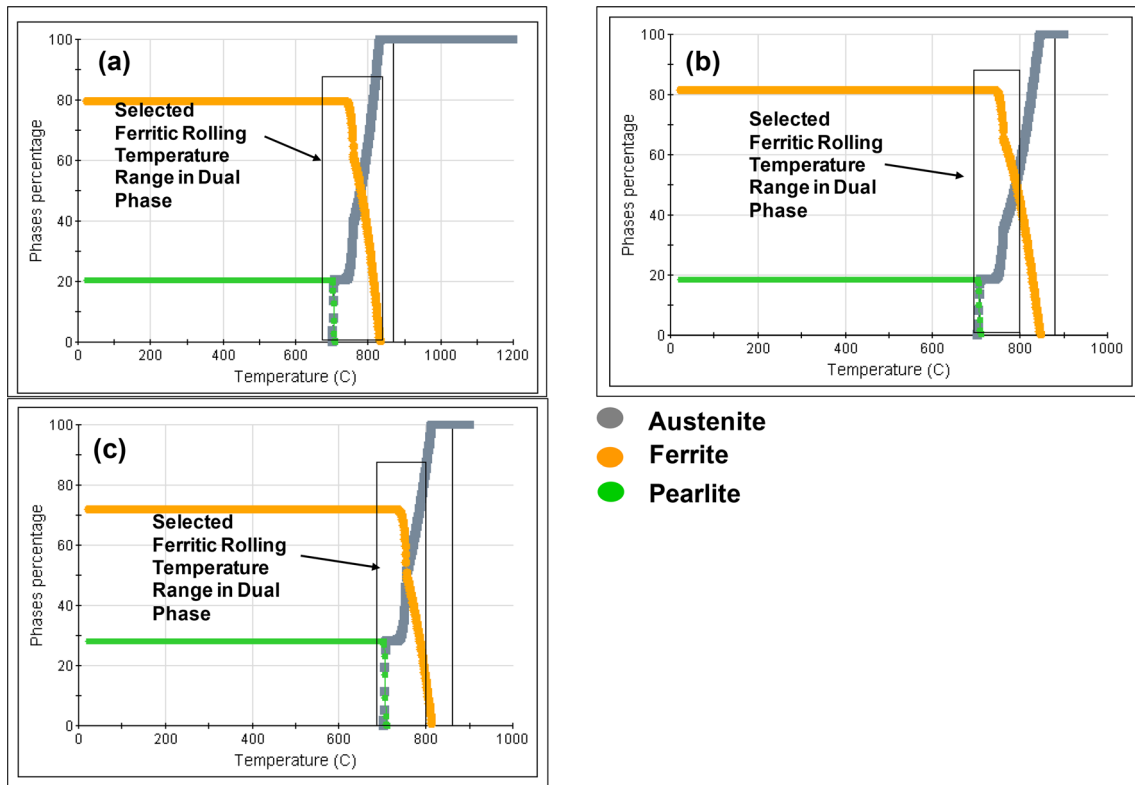
#### 3.3 Analysis of $r$ Values

Figure 7 presents the  $r$  values of the steels in hot rolling and warm rolling conditions of E450 grade steel. After rolling in both conditions, the steel presents  $r$  values near to 1 irrespective of hot rolling temperature. Some deleterious effect is observed while rolling in the ferritic region; the warm-rolled steel shows more negative values of planar anisotropy ( $\Delta r = -0.6$ ) in comparison with hot-rolled steel ( $\Delta r = -0.015$ ). The negative values can be attributed to the banded structure observed in warm-rolled steel which has given rise to anisotropy in properties. However,  $\Delta r$  value has been found to change with hot rolling temperatures [13]. The  $r$  values (with standard deviation) in tabular form are shown in Table 4.

#### 3.4 Deformation Map

Deformation maps are extensively used to determine the optimum process parameters without trial and error and determine process limitations in the manufacturing process [11, 12]. Prasad et al. developed the deformation map based on the theory of the Dynamic Material Model (DMM) [13] assuming the power-law relationship between flow stress  $\sigma$  and strain rate  $\dot{\epsilon}$ . The strain rate sensitivity ( $m$ ) determines the amount of power dissipated through deformation and microstructure changes. The  $m$  is expressed as given in Eq. (1):





**Fig. 5** Phase percentage versus temperature of the selected grade **a** E250 **b** E350 and **c** E450

$$m = \left[ \frac{\partial J}{\partial G} \right]_{\varepsilon, T} = \frac{\partial \ln \sigma}{\partial \ln \dot{\varepsilon}} \Big|_{\varepsilon, T} \quad (1)$$

The power dissipation characteristics by microstructural changes under different temperature and strain rates are represented in terms of efficiency ( $\eta$ ) and are defined as Eq. (2):

$$h = J/J_{\max} = 2m/(m+1) \quad (2)$$

The plot of  $\eta$  with respect to temperature and strain rate is known as power dissipation map. Further, flow instability parameter ( $\xi$ ) representing metallurgical instability is determined and superimposed with power dissipation map to constitute the deformation map along with the power dissipation map.  $\xi$  is determined using Eq. (3).

$$\xi(\dot{\varepsilon}) = \frac{\partial \ln \left( \frac{m}{m+1} \right)}{\partial \ln \dot{\varepsilon}} + m < 0 \quad (3)$$

Flow stresses at different strain rates and deformation temperatures have also been determined using JmatPro and used for constructing the deformation map. Based on the computation of strain rate sensitivity and in turn efficiency of power dissipation during deformation, complete processing maps for all the three grades have been constructed for 0.5 strains as shown in Fig. 8a–c. The

continuous line shows an iso-efficiency contour and the instable region is indicated by the shaded region. The deformation map indicates that the processing of all the selected three grades is safe in the temperature range of 700–900 °C and with a lower strain rate. Thus, the deformation map also aided in deciding the rolling parameters of the identified grades.

### 3.5 Mill Load During Warm Rolling

To evaluate the effect of deformation temperature on mill load, the draft schedule and total reduction were kept the same in all the experiments. The mill load was measured using load cell (Model No- SC015H9) installed in ERM. The deviation in load measurement found to be  $\pm 1$  ton. The first experiment was carried out at 900 °C (100% austenite phase) depicting hot rolling conditions and taken as a reference for other experiments. Since the reduction was kept highest in pass No-1, the maximum rolling load was observed in this pass compared to subsequent passes. The rolling load obtained in pass No-1 was compared and shown in Fig. 9 for E-350 grade steel. It can be seen that, mill load is 77 tons at a deformation temperature of 900 °C and it increases to 80 tons at a deformation temperature of 800 °C. The increase in mill load is nominal by reducing the rolling temperature to 760 °C and 730 °C. It can be

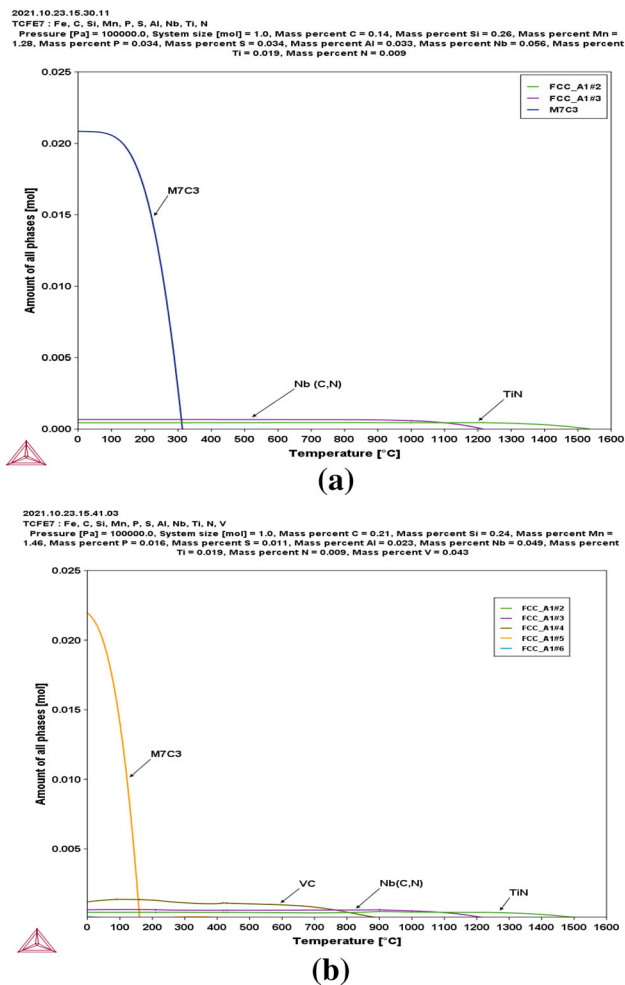


Fig. 6 a, b are plots drawn through Thermo-Calc of the amount of phases with respect to temperature for steels Nb–Ti and Nb–V–Ti

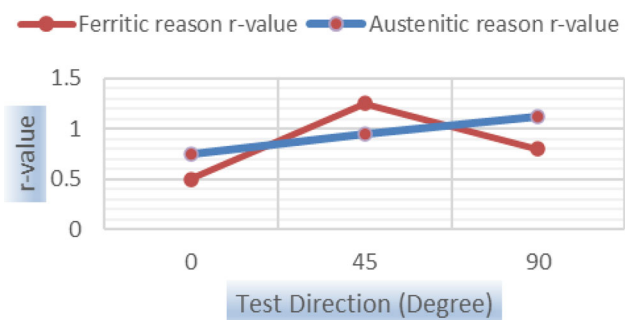


Fig. 7 Measured  $r_m$  normal anisotropy values for E450 Steel

Table 4  $r$  values in hot and warm rolling

Rolling	0°	45°	90°
Ferritic region	0.50 ± 0.08	1.25 ± 0.14	0.80 ± 0.13
Austenitic region	0.75 ± 0.11	0.95 ± 0.11	1.12 ± 0.09

seen that increase in mill load from hot rolling to warm rolling temperature is not significant, since rolling is performed in a single-phase region. However, the mill load increases significantly to 91 tons as the deformation temperature is reduced to 710 °C due to the presence of the pearlite phase at this temperature. A similar trend in mill load was observed in the other two grades also.

The mill load obtained in the first pass for the three experimental steel is shown in Fig. 10. Figure 10 depicts the mill load for experimental steels at deformation temperature where more than 90% ferrite is formed as per JMatPro analysis. It reveals that, the mill load increases as micro-alloying increases in the steel. It can be seen that the mill load obtained during warm rolling of E250 grade at the temperature (< 780 °C) is around 70 tons. The mill load increases by 20–30% during warm rolling of micro-alloyed steel compared to E250 grade. Thus, higher mill capabilities will be required for warm rolling of micro-alloyed steel during industrial-scale trials.

### 3.6 Microstructural Analysis

#### 3.6.1 Optical Microscopy

Optical microscopy was carried out to understand the effect of warm rolling on microstructures. The detailed microstructures of the warm-rolled samples are shown in Fig. 11. Figure 11a shows the microstructures of E250 grade steel hot rolled at 780 °C having ferritic grain size 7.5 μm. Here more than 90% of the microstructure is ferrite, and the structure is fine due to the recrystallization of ferrite. Figure 11b shows the microstructure of E250 grade steel rolled at 740 °C having grain size around 11 μm, which is partially recovered and recrystallized due to rolling at a lower temperature. Microstructures also show elongated ferrite and pearlite with the presence of fragmented pearlite. Microstructures of E350 grade steel rolled at 900, 760, and 710 °C are shown in Fig. 11c–e. At a higher temperature of 900 °C, the microstructure is ferrite and pearlite having grain size 10.2 μm and that is completely recrystallized. It seems that the grains rolled at 900 °C are coarser than E250 grade steel rolled at 780 °C due to the higher temperature of rolling. While, with lower temperature, elongated ferrite, and fragmented pearlite is

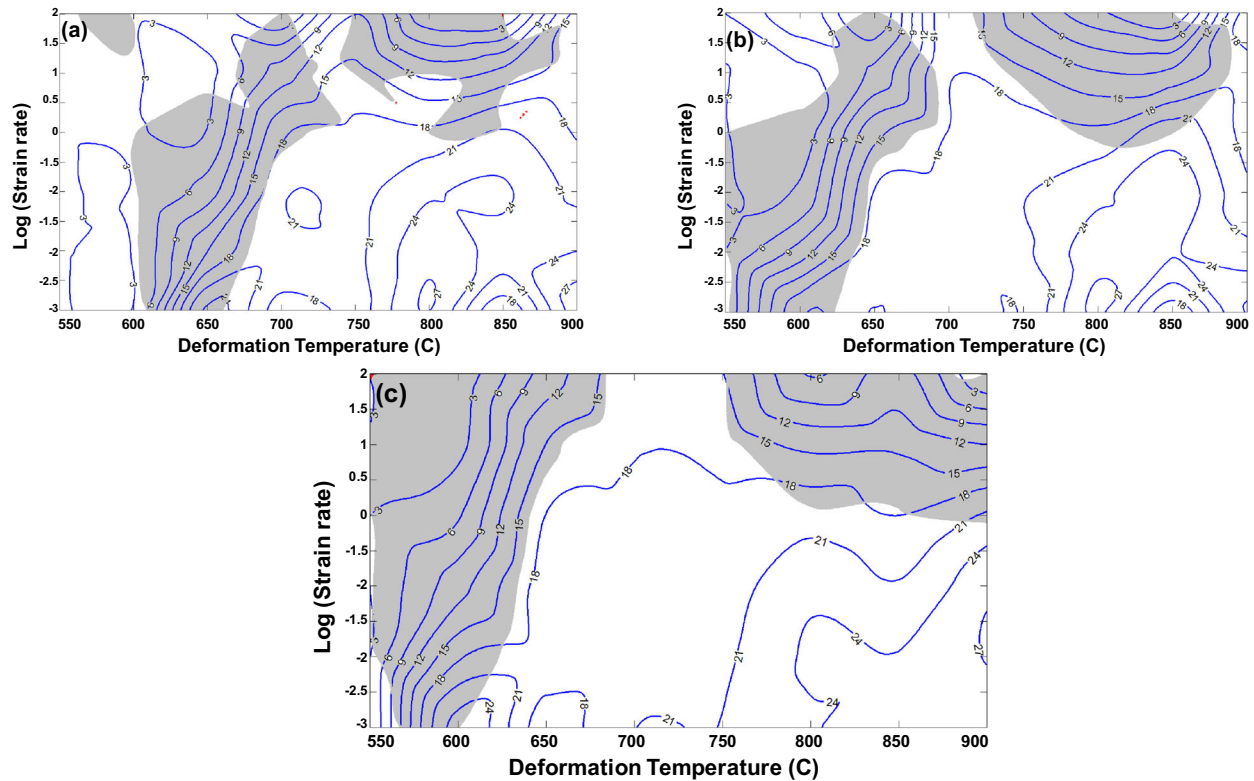


**Fig. 8** Deformation Map a E250 b E350, and c E450

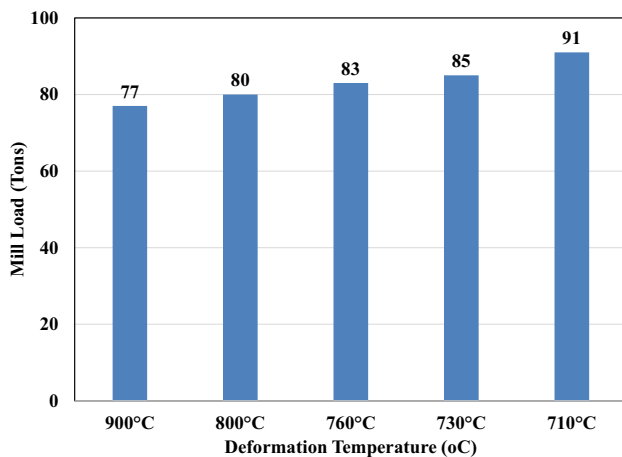


**Fig. 9** Mill load obtained during warm rolling (deviation in measurement  $\pm 1$  ton)

formed due to a lesser degree of recovery and minor recrystallization. At 760 °C, the maximum grains are recrystallized and a few grains are elongated. The elongated grains are mainly due to dynamic recovery (DR) as it is the main mechanism during warm rolling as the stored energy required for Continuous Dynamic Recrystallization (CDRX) is not adequate [3]. As the temperature is further decreased, i.e., at 710 °C the grains are partially recrystallized and the majority of grains are elongated as DR has

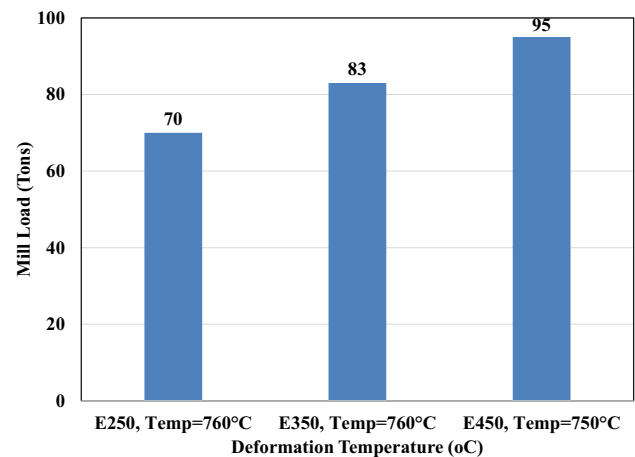


**Fig. 10** Mill load obtained in first pass of rolling (deviation in measurement  $\pm 1$  ton)

predominantly occurred. The grain size of warm-rolled experimental steel is shown in Table 5. The pearlites are more fragmented compared to E250 grade steel at lower temperatures. Shen et al. reported that CDRX of a 0.0016C-0.1Si-0.3Mn (wt%) was induced in a single pass warm rolling process at a low strain rate ( $0.01 \text{ s}^{-1}$ ) and high temperature but CDRX was inhibited at a relatively high strain rate ( $1 \text{ s}^{-1}$ ) and lower temperature [14]. In the present case, warm rolling was performed at higher strain



**Fig. 11 a, b** Optical Micrographs of E250, Rolled at 780 & 740 °C, Air cooling, **c–e** Optical Micrographs of E350, Rolled at 900, 760 & 710 °C, Air cooling, **f, g** Optical Micrographs of E450, Rolled at 800 & 710 °C, Air cooling

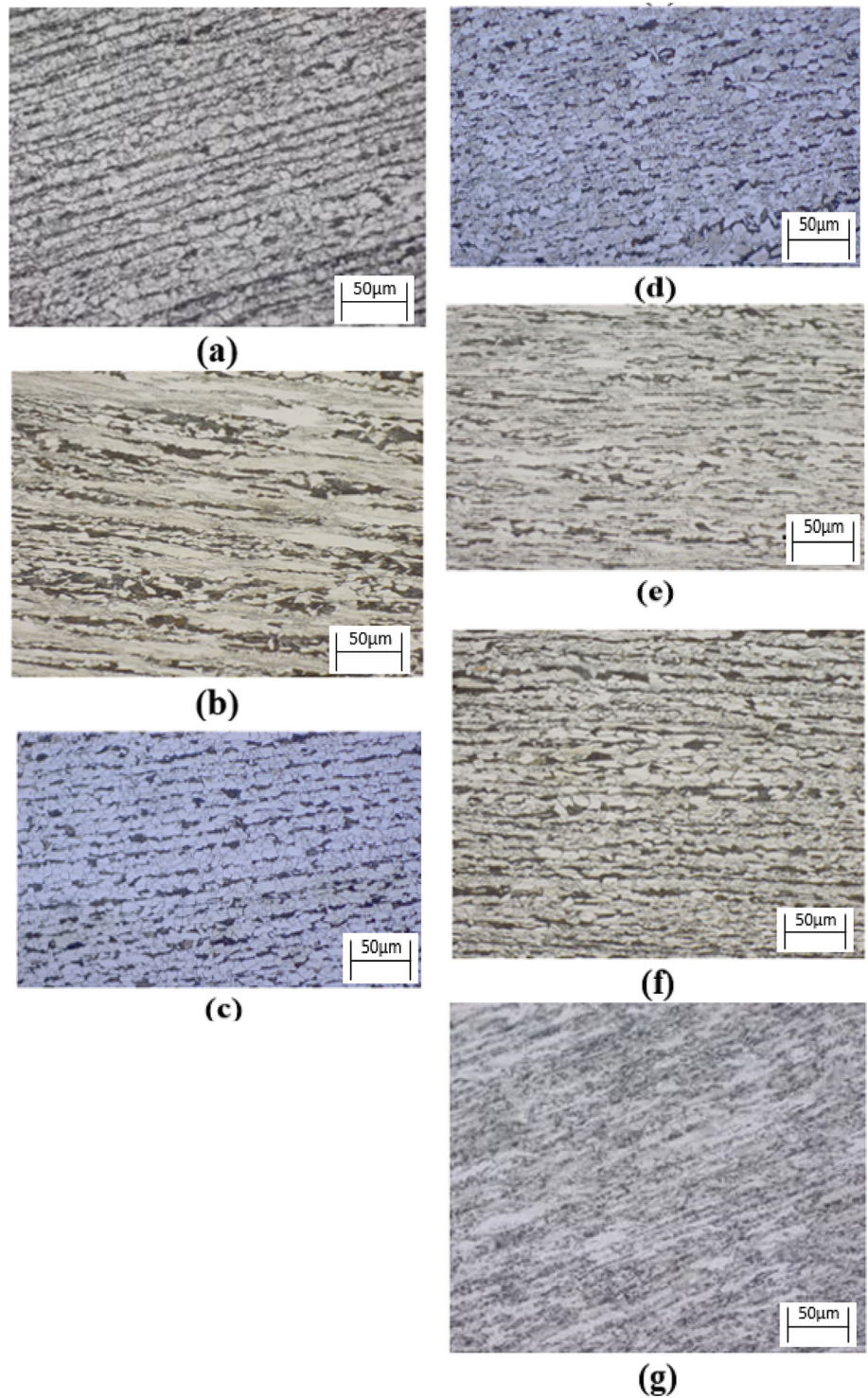


**Table 5** Grain size of steel as per finish rolling temperature

Steel	Ferrite grain size	Ferrite grain size
E250	7.5 ± 0.9 µm (780 °C)	11 ± 1.7 µm (740 °C)
E350	10.2 ± 1.2 µm (900 °C)	9.8 ± 0.9 µm(760 °C)
E450	9.7 ± 1.4 µm (800 °C)	5 ± 0.7 µm (710 °C)

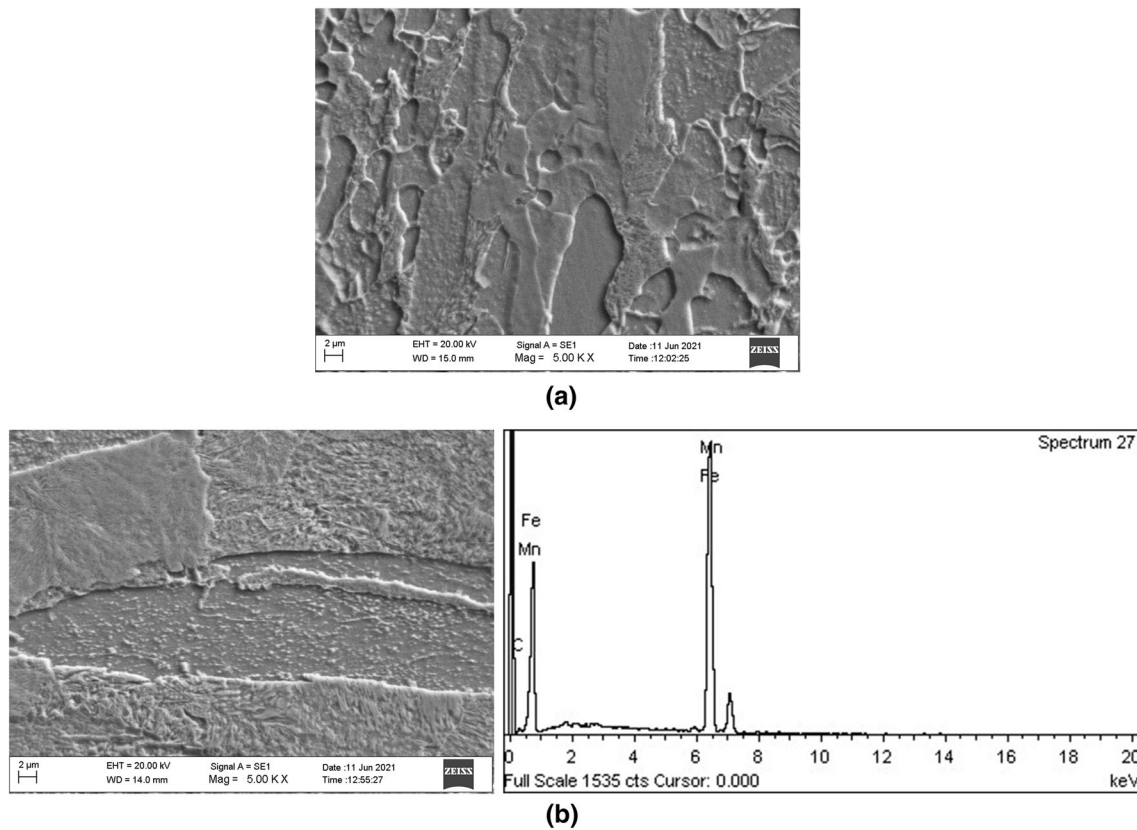


**Fig. 12** SEM micrograph of E250 steel grade finish rolled at **a** 780 °C and **b** 740 °C and air-cooled, **b** also having EDS spectrum related to steel finish rolled at 740 °C

rates ( $> 15 \text{ s}^{-1}$ ), thus the CDRX phenomenon was inhibited and the grains were found to be elongated and pearlites found to be fragmented.

In the case of E450 grade, the fragmentation at a lower temperature of 750 °C is more compared to higher temperature rolling at 800 °C. At higher temperatures, there seems to happen both DR & CDRX and the grains are more refined. At lower temperatures due to no recrystallization and low diffusion, the fragmentations of pearlites and ferrites are more elongated and finer. Also, a lesser degree of recrystallization happens in E450 grade steel due to the pinning effect by lower temperature precipitates of VC. The Nb, Ti (C,N), and VC precipitates were observed through EDS in the TEM section of this paper in E450 grade steel. Microstructures of E450 grade steel rolled at 800 and 710 °C are shown in Fig. 11f–g. Among the three grades, the E450 grade has more strength due to finer and more elongated ferrite along with more fragmentation in Pearlite with finer size.

It is worth mentioning that the effect of hot rolling is significant in grain size but warm rolling is not as significant as hot rolling. The precipitates of Nb, Ti (C,N) are being supportive to refine grain size during hot rolling. The grains during warm rolling are coarser than hot rolling due

to only dynamic recovery (DR) as having lesser stored energy in the form of stacking fault energy for further recrystallization.

### 3.6.2 Scanning Electron Microscopy

Figures 12a, b show the scanning electron micrographs of E250 grade steel finish rolled at 780 °C and 740 °C, respectively, and corresponding EDS analysis result of steel rolled at 740 °C. In E250 grade steel, higher-finish rolling temperature shows predominantly polygonal ferrite and fragmented pearlite structure (ferrite + spheroidal cementite). At finish rolling temperature, i.e., at 740 °C, grain shear bands are seen which has caused fragmentation of warm-rolled structure resulting in predominant elongated ferrites. This has led to higher strength as compared to the higher-finish rolling temperature at 780 °C [15]. The fragmented pearlite as generated by warm rolling, is being confirmed by the EDS spectrum as shown in Fig. 12b.

Figure 13a–c shows the scanning electron micrographs of E350 grade steel finish rolled at 900 °C, 760 °C, and 710 °C, respectively. The microstructure of E350 grade at higher-finish rolling temperature, i.e., at 900 °C, shows predominantly polygonal ferrite, few pearlites, and

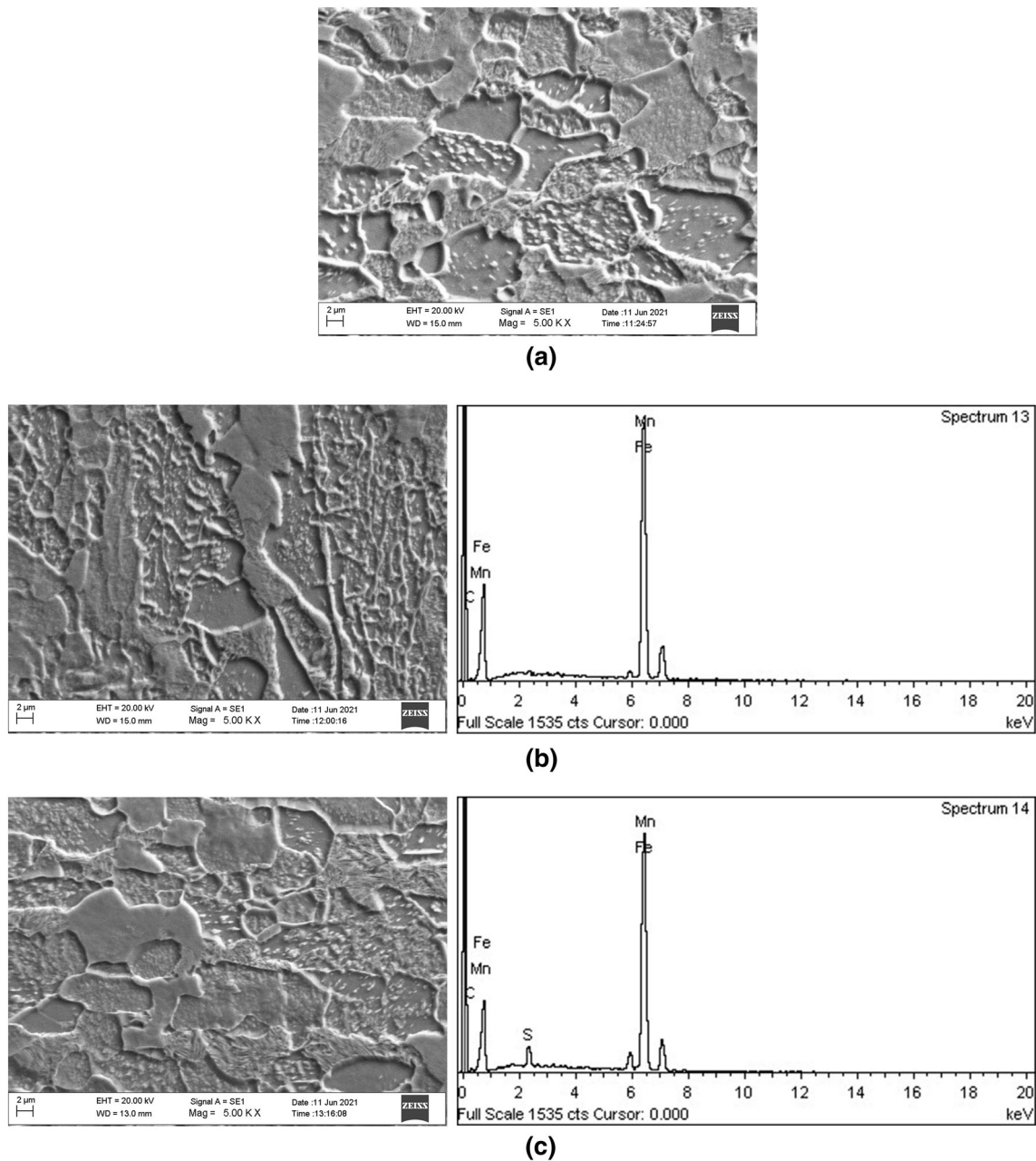


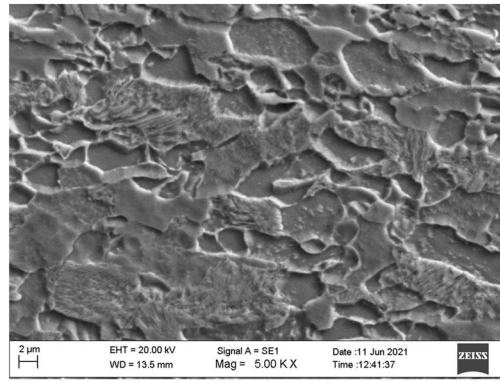
**Fig. 13** SEM micrographs of E350 steel grade finish rolled at **a** 900 °C and **b** 760 °C, and **c** 710 °C and air-cooled, **b** & **c** also having EDS spectrum related to steel finish rolled at 760 °C & 710 °C

fragmented pearlite structure (ferrite + spheroidal cementite). As the temperature of finish rolling is decreased, the percentage of fragmented pearlite is increased. Hence, fragmented pearlites are more predominant at a lower finish temperature of 710 °C. The fragmented pearlite is being confirmed by EDS spectrum as shown in Fig. 13b, c, rolled at lower temperatures 760 °C and 710 °C. This resulted in higher strength in comparison with a higher rolling temperature of 900 °C. The grains are more refined in E350 grade steel than E250 grade steel due to having micro-alloying elements Nb and Ti in steel which hinders

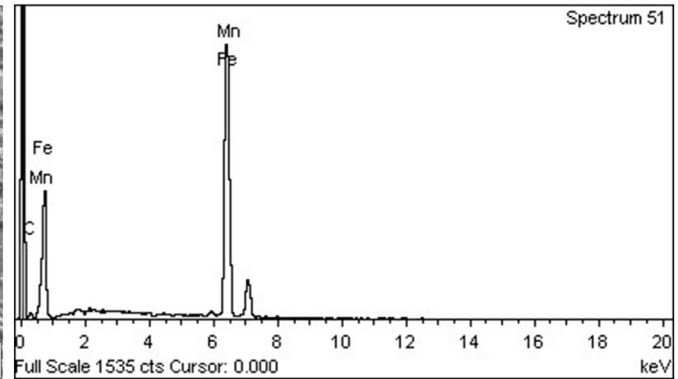
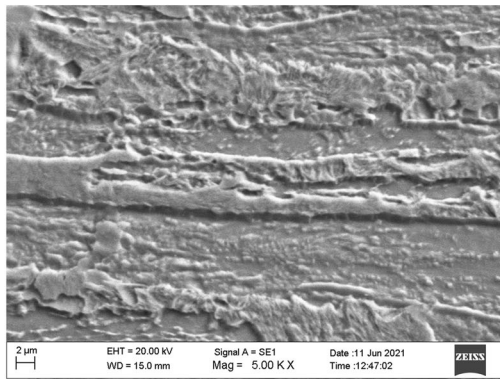
austenite grain coarsening by pinning effect by its precipitates like Nb, Ti (CN), and TiC.

Figures 14a–c shows the scanning electron micrographs of E450 grade steel finish rolled at 800 °C, 750 °C, and 710 °C, respectively. The microstructure of E450 grade at higher-finish rolling temperature, i.e., at 800 °C shows predominantly polygonal ferrite, pearlite structure, and fewer percentage of fragmented pearlites. As the temperature of finish rolling is decreased, ferrite and fragmented pearlite become predominant. The fragmented pearlite concentration is being increased with decreasing

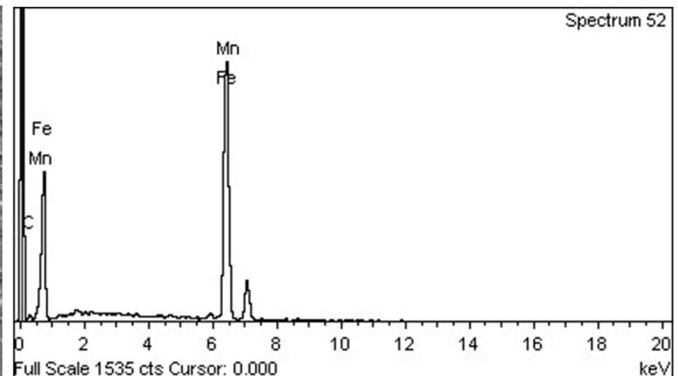
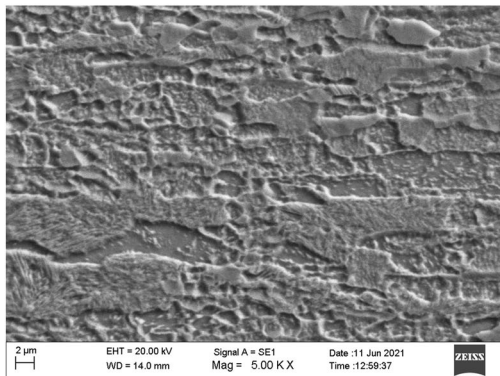




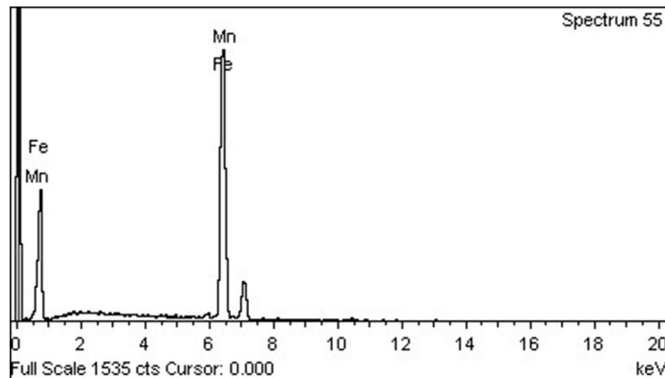
(a)



(b)



(c)



(d)

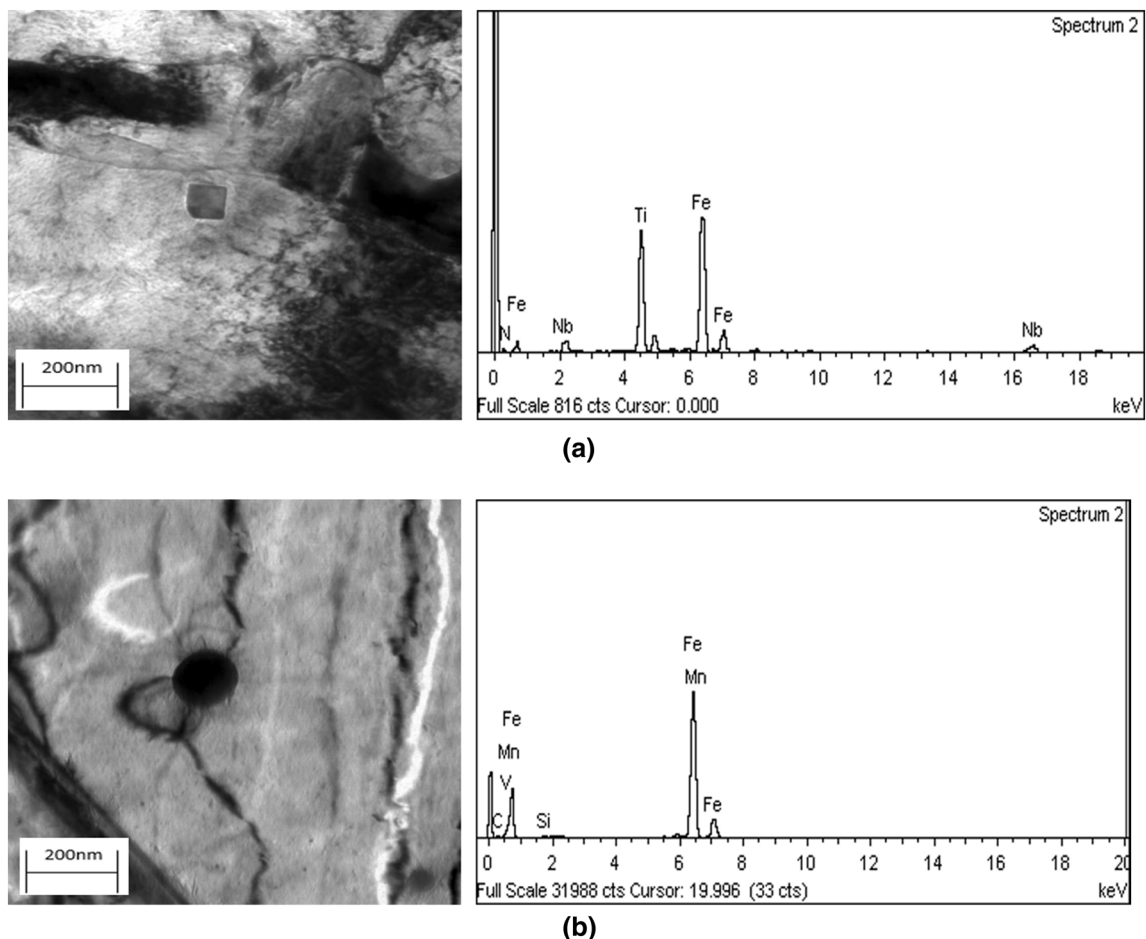
◀ **Fig. 14** a–c SEM micrographs and EDS spectrum of E450 grade steel finish rolled at a 800 °C and b 750 °C c 710 °C and air-cooled, b, c also having EDS spectrum related to steel finish rolled at 750 °C & 710 °C, and d EDS spectrum of ferrite region of fragmented pearlite

temperature. Hence, the ferrite and fragmented pearlites are more predominant at a lower temperature of 710 °C. This has led to higher strength in comparison with a higher-finish rolling temperature of 800 °C. As a normal phenomenon in E450 grade steel, the fragmented pearlite should be lesser in comparison with E250 and E350 grade steel due to consumption of C by precipitation of carbides of Nb, V, and Ti, but in the case of E450 grade, more fragmented pearlite is observed due to higher percentage of C (0.21%) in steel [15]. Finer elongated and finer fragmented pearlite in E450 grade helped in achieving higher strength in comparison with E250 and E350 grades. The EDS spectrum related to cementite and ferrite has been

shown in Fig. 14b, c, which confirms the appearance of fragmented pearlite generated during warm rolling in E450 grade steel. Figure 14d shows EDS spectrum taken within fragmented pearlite of ferrite portion that also confirms about fragmented pearlite.

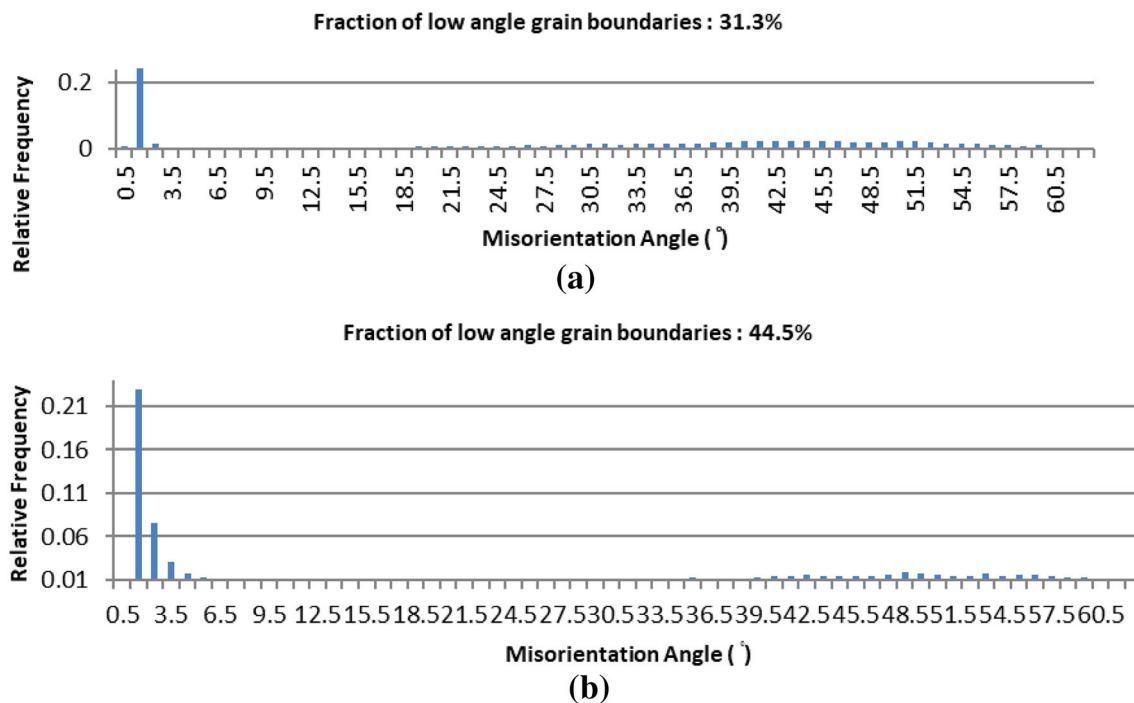
### 3.6.3 Transmission Electron Microscopy (TEM)

Figure 15 shows TEM micrographs of the E450 and types of precipitate during warm rolling. There is a high density of dislocations in the matrix of elongated ferrite, as shown in Fig. 15a. The EDX analysis shows two types of precipitates: Niobium Carbonitrides and Vanadium Carbides as shown in Fig. 15a, b. Niobium Carbonitrides, i.e., Nb, Ti (C, N) precipitates of around 80 nm have been formed at higher temperatures, i.e., during hot rolling. The second category of precipitates, i.e., Vanadium Carbide (VC) of size 100 nm with spherical shaped morphology are formed at lower temperature, i.e., during warm rolling. The results show that the Nb, Ti (C, N) particles precipitate first and VC precipitates later. The precipitates in Nb–Ti steel



**Fig. 15** Transmission electron micrograph showing carbides in steel a, b bright field image of precipitates of Nb,Ti(C,N) and VC and its EDS spectrum





**Fig. 16** Misorientation distribution of steels deformed at **a** RT = 800 °C (hot rolling), and **b** RT = 710 °C (warm rolling)

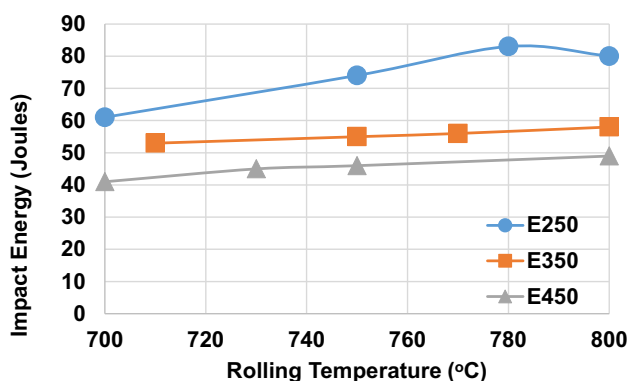


**Fig. 17** Variation of impact energy with rolling temperature (standard deviation in measurement:  $\pm 1.85$  J)

(E350) and Nb–V–Ti (E450) steel have a similar feature of morphology. From the EDX analysis of E450, it is observed that the VC precipitates due to higher carbon content in steel and this also confirms the Thermo-Calc analysis. VC seems to hinder the precipitation of ferrite and hence results in the formation of elongated ferrites.

### 3.6.4 Electron Back-Scattered Diffraction (EBSD)

Figure 16a, b shows grain boundary misorientation distribution of E450 warmed rolled plates at 800 and 710 °C, respectively. The fraction of High-Angle Grain Boundaries (HAGBs) has been found to be more at 800 °C compared to 710 °C. Fraction of HAGBs decreases at a lower

temperature, because of a decrease in recrystallized ferrite and more dislocation induced during warm rolling.

Significant grain refinement is obtained during warm rolling of micro-alloyed steel (E450) with grain size found  $\sim 5$   $\mu\text{m}$  at the lower temperature of 710 °C. This lead to an improvement in tensile properties according to the Hall–Petch relationship. An increase in low-angle grain boundaries due to the DR mechanism at lower temperature also indicates that dislocation strengthening has led to increased strength by warm rolling. Thus, reducing warm rolling temperature remarkably improves the strength of the warm-rolled plates.

### 3.7 Mechanical Testing

The toughness of the ferrite-rolled samples was evaluated by the Charpy test at room temperature. The standard deviation in measurement during Charpy test has been found to be  $\pm 1.85$  J. Marginal drop in impact energy is observed for E-250 grade when rolled at a lower temperature compared to a higher temperature warm-rolled samples as shown in Fig. 17. Flatter curves are observed for micro-alloyed steels as shown in Fig. 17. This indicates that rolling in a warm zone does not adversely affect the toughness of the micro-alloyed steel. Further, it has been confirmed that banded structure in E250 grade steel leads to more drop-in toughness values when warm rolling is done, while in E350 and E450 steel, the drop in toughness values as the temperature is being decreased is less in

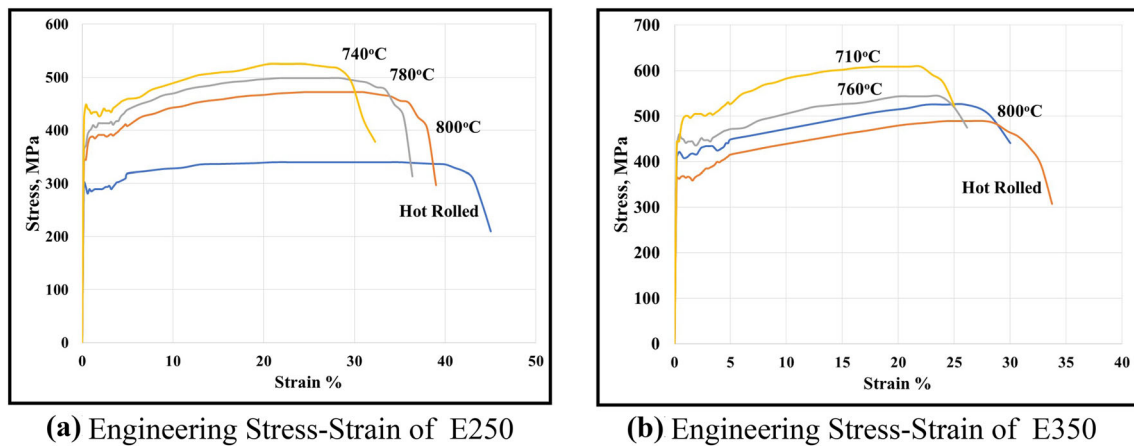


**Fig. 18** a Engineering Stress–Strain of E250 b Engineering Stress–Strain of E350

comparison with warm rolling of E250 due to not having banded structure.

Yield strength (YS) and Ultimate Tensile Strength (UTS) of warm-rolled samples were evaluated in the rolling direction. Figure 18a shows the engineering stress–strain curves of warm-rolled plates for E250 grade steel.

It can be seen that YS and UTS achieved are 385–455 MPa and 470–525 MPa, respectively, during warm rolling is much higher than the required value of 250 MPa and 410 MPa respectively. The percentage elongation is achieved in the range of 26–30, which is less than the conventionally hot-rolled samples but meet the grade requirement. Engineering stress–strain curves of E350 grade are shown in Fig. 18b. YS and UTS of E350 of warm-rolled samples are found to be in the range of 399–450 MPa and 500–610 MPa. Thus, it can be seen that warm rolling improves strength, however, there is a marginal drop in the ductility; however, it meets the grade requirement. Similar results have also been achieved in E450 grade steel. The microstructure in this temperature range is composed of more than 90% of ferrite and results in improved mechanical properties due to warm rolling. With these results, it can be inferred that, warm rolling can be used to achieve higher strength and toughness properties with the same alloy chemistry.

#### 4 Conclusions

- The mill load obtained during warm rolling of E250 grade has been found to be lower compared to that of micro-alloyed grades E350 and E450. Thus, trials for warm rolling on an industrial scale can be taken up with the existing mill capability. Warm rolling of micro-alloyed steel may require higher mill capacity due to an increase in mill load by rolling at a lower temperature.

- The microstructure of warm-rolled samples reveals elongated ferrite along with fragmented pearlite indicating most of the reduction has occurred after  $A_{r1}$  temperature. As the temperature is being decreased, ferrite and fragmented pearlites are being fine and the elongation in ferrite and fragmentation in pearlites are being more. Finer grains and more fragmentation in pearlites can be the major reason for improved strength in the warm-rolled samples.
- The results obtained in experimental steels confirm that improved mechanical properties can be achieved with warm rolling with the same alloy chemistry. The yield strength of the warm-rolled sample has been found to be a minimum 10% higher than the conventional hot-rolled sample without impairing the toughness properties.
- The warm rolling has resulted in more negative values of planar anisotropy ( $\Delta r = -0.6$ ) in comparison with hot-rolled steel ( $\Delta r = -0.015$ ). The more negative values can be attributed to the banded structure observed in warm-rolled steel which has given rise to anisotropy in properties.

**Acknowledgements** The authors are grateful to the management of RDCIS, Ranchi for their continued patronage during the execution of the project. They are also thankful to all the laboratory personnel who have helped in conducting various tests during the execution of the project.

#### References

1. H. Bin, T. Xin, H. Luo, X. Mao, *J Mater Sci Technol [J]* **47** (2020) 131.
2. H. Bin, *Acta Mater* **174** (2019) 131.
3. H. Zheng, L. Fu, Z. Li, X. Ji, Q. Wang, W. Wang, A. Shan, *Mater Today Commun* **20** (2019) 100565 <https://doi.org/10.1016/j.mtcomm.2019.100646>
4. T. Inoue, *Mater Sci Eng A* **786** (2020) 139

5. H. Jun, D. Lin-Xiu, H. Xie, Y. Peng, R.D.K. Misra, *Mater Sci Eng A* **605** (2014) 186.
6. B. Gao, Q. Lai, Y. Cao, H. Rong, L. Xiao, Z. Pan, N. Liang, Y. Li, G. Sha, M. Liu, H. Zhou, W. Xiaolei, Y. Zhu, *Sci Adv* **6** (2020) eaba8169
7. X.J. Shen, S. Tang, Y.J. Wu, X.L. Yang, J. Chen, Z.Y. Liu, R.D.K. Misra and G.D. Wang, *Mater Sci Eng A* **685** (2017) 194 <https://doi.org/10.1016/j.msea.2016.12.108>
8. S.N. Sergeev, I.M. Safarov, A.V. Korznikov, R.M. Galeev, S.V. Gladkovsky, D.A. Dvoynikov, *Lett Mater* **5** (2015) 48.
9. Y.W. Kim, J.H. Kim, S.-G. Hong, C.S. Lee, *Mater Sci Eng A* **605** (2014) 244.
10. D.S. Kumar, M. Sambandam, U. Bhat, *Iron Mak Steelmak* **47** (2020) 632. <https://doi.org/10.1080/03019233.2020.1793290>
11. M.S. Popkiadeh, A Rezaeian, G Dini, M R Toroghinejad, *ISIJ Int* **55** (2015) 691.
12. S.K. Thakur, L. Harish, A.K. Das, S. Rath, P. Pathak, B.K. Jha, *Mater Today: Proc* **28** (2020) 1973.
13. Y. Prasad, T. Seshacharyulu, *J Int Mater Rev* **43** (1998) 243.
14. X.J. Shen, S. Tang, Y.J. Wu, X.L. Yang, J. Chen, Z.Y. Liu, R.D.K. Misra, G.D. Wang, *Mater Sci Eng A* **685** (2017) 194.
15. G.H. Akbari, C.M. Sellars, J.A. Whiteman, *Acta Mater* **45** (1997) 5047.

**Publisher's Note** Springer Nature remains neutral with regard to jurisdictional claims in published maps and institutional affiliations.